Digitally Programmable Fully Differential Filter

Parveen BEG[1], Iqbal A. KHAN[2], Sudhanshu MAHESHWARI[1], Muzaffer A. SIDDIQI[1],

[1] Dept. of Electronics Engineering, Aligarh Muslim University, Aligarh, 202002, India
[2] Dept. of Electrical Engineering, Umm Al Qura University, P.O. Box: 5555, Kingdom of Saudi Arabia

parveenbeg@gmail.com, iakhan@uqu.edu.sa, sudhanshu_maheshwari@rediffmail.com, masamu@rediffmail.com,

Abstract. *In this paper a new digitally programmable voltage mode fully differential Kerwin-Huelsman-Newcomb (KHN) filter is realized using digitally controlled CMOS fully balanced output transconductor (DCBOTA). The realized filter uses five DCBOTAs, a single resistor and two capacitors. The filter provides low-pass, high-pass and band-pass responses simultaneously. The pole-frequency of all the responses is controlled by externally applying an 8-bit digital control word. All the responses exhibit independent digital control for pole-ω_0 and pole-Q. The proposed filter also offers low passive sensitivities. Non-ideal gain and parasitic associated with the actual DCBOTA is also discussed. The CMMR results for low-pass response are also included which highlight the advantage of a fully-differential operation. Exhaustive PSPICE simulation is carried out using 0.5μ technology which may be further scaled to explore state-of-the-art applications of the proposed circuit.*

Keywords

Fully Differential, Digital Control, KHN Filter.

1. Introduction

Fully differential circuit configurations have been widely used in high frequency analog signal processing applications like new-standard wireless receivers [1]. As compared to their single ended counterparts, they exhibit a higher capability to reject power supply noises, and offer a large output dynamic range along with reduced harmonic distortion. A number of fully differential biquad filter circuits based on active elements have been reported in literature [2]-[4]. However, they require a large number of passive components. The differential KHN using dual output differential difference current conveyor (DO-DDCCs) [2] uses three DO-DDCCs, two capacitors and five resistors. The circuit in [3] includes three FDCCII, six resistors and four capacitors. The design proposed in [4] has three FDCCII, four floating resistors and two floating capacitors. Both the circuits i.e. within [3] and [4] are capable of generating only low-pass and band-pass responses. In contrast, the circuit proposed within this article is composed of five active elements, namely DCBOTAs along with only two capacitors and one resistor. In addition, the circuit also provides programmable high-pass, band-pass and low-pass responses.

Operational transconductance amplifier (OTA) is widely used in the design of electronically tunable analog filters. Several realizations of CMOS transconductors with single or multiple outputs along with their applications have been reported [5]-[8]. The OTA based filters reported in [5], [7] provides all responses but no independent tuning between pole-frequency and pole-Q. Several KHN filters based on different active device have also been reported, but with single-ended input-output configurations [9]-[11].

Digitally controlled CMOS fully balanced output transconductor (DCBOTA) is useful building block for the design of digitally programmable filter. Filters [12]-[14] based on DCBOTA are also available. But none of the configurations is fully differential. Filter [12] gives low-pass and band-pass responses and the one in [13] produces band-pass response. Recently a digitally programmable current mode filter based on DVCC was also introduced [15], in which the filter responses were digitally selected using built in CMOS switches.

In this paper, a new voltage mode digitally programmable fully differential KHN (DP-FDKHN) filter with minimum passive components is presented. The filter employing digitally controlled CMOS fully balanced output transconductor as an active element [12] is used. The digital control of the DCBOTA is achieved using a current division network (CDN) [12], [16], [17]. The CDN to be used in this work is from [12]. It exhibits features such as independent digital control of pole-ω_o and pole-Q through a control word, low sensitivity figures and a wide frequency range. The realized DP-FDKHN was designed and simulated using PSPICE.

2. Circuit Description

The electrical symbol of DCBOTA as proposed in [12] is shown in Fig. 1.

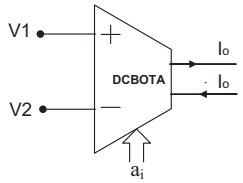

Fig. 1. Electrical symbol of DCBOTA.

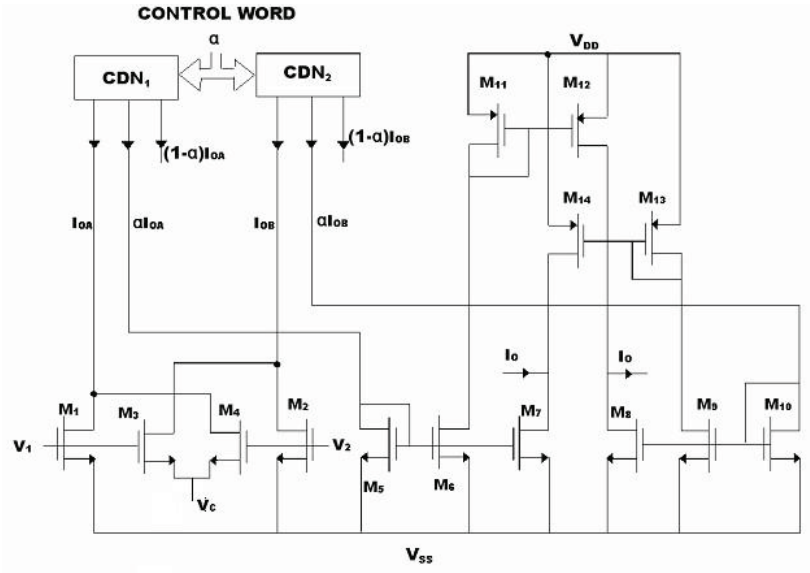

Fig. 2. CMOS realization of DCBOTA [12].

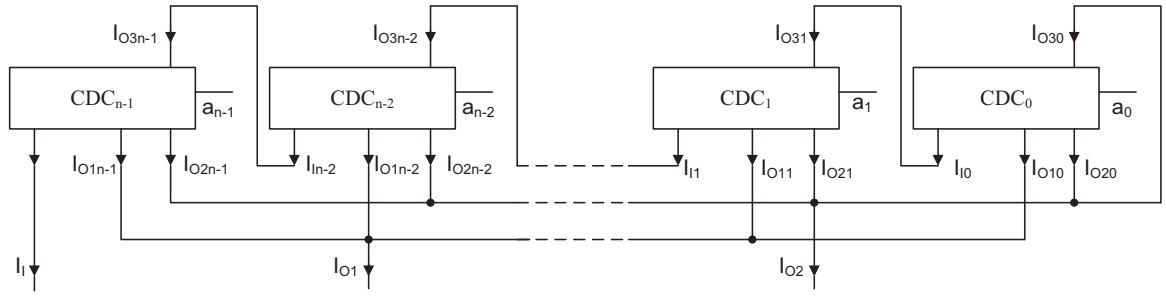

Fig. 3. Block diagram of CDN [12].

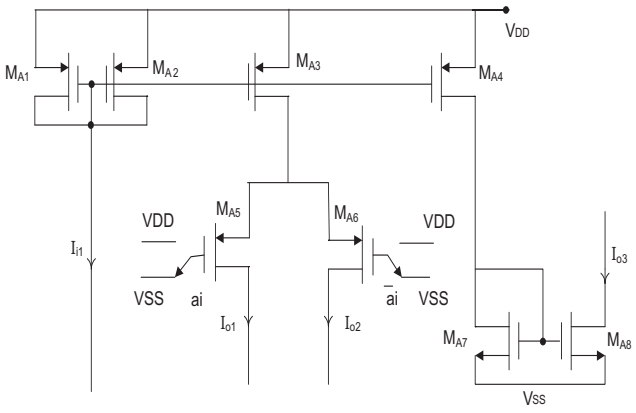

Fig. 4. CMOS realization of CDC [12].

The CMOS realization of the DCBOTA is shown in Fig. 2. The MOS drain current in the saturation is given by

$$I_o = \alpha K\left(V_C - V_{SS}\right)\left(V_1 - V_2\right). \tag{1}$$

Therefore, the DCBOTA circuit operates as a digitally controlled balanced output transconductor with programmable transconductance G_m which, in turn, is controlled by the digitally controlled parameter α. This is represented as

$$G_m = \alpha K\left(V_C - V_{SS}\right) \tag{2}$$

where

$$K = \mu_n C_{ox}\left(W/L\right),$$

$\left(W/L\right)$ = transistor aspect ratio,

μ_n = electron mobility,

C_{ox} = gate oxide capacitance per unit area.

Digital control parameter α is actually realized using a current division network shown in Fig. 3. It consists of n current division cells (CDCs) as shown in Fig. 4.

The output currents of the CDN are given as

$$I_{O1} = \alpha I_1, \tag{3}$$

$$I_{O2} = \left(1-\alpha\right) I_1, \tag{4}$$

$$\alpha = \frac{I_{O1}}{I_1} = \frac{1}{2^n}\left(\sum_{i=0}^{n-1} 2^i a_i\right) \tag{5}$$

where $a_i = [a_7\ a_6\ a_5\ a_4\ a_3\ a_2\ a_1\ a_0]$ is the digital control word which can be applied to CDN externally.

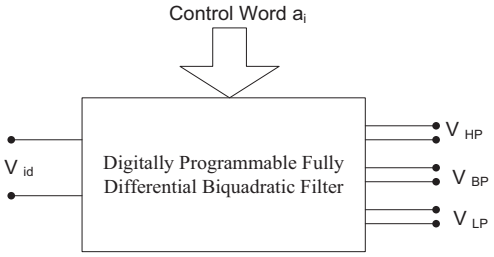

Fig. 5. Block diagram representation.

The DCBOTA is used to convert the well known KHN filter into a digitally programmable fully differential KHN filter. The block diagram of the proposed biquadratic filter is shown in Fig. 5. It uses five DCBOTAs, two capacitors and a single resistor as shown in Fig. 6. Tuning of this filter is achieved by using the digitally controlled word.

Analysis of the proposed filter yields the transfer function as

$$\frac{V_{HP}}{V_{id}} = \frac{V_{O3} - V_{O4}}{V_{id}} = \frac{s^2 \left(G_{m1} R\right)}{D(s)}, \tag{6}$$

$$\frac{V_{BP}}{V_{id}} = \frac{V_{O5} - V_{O4}}{V_{id}} = \frac{s\left(\frac{G_{m1} G_{m4} R}{C_1}\right)}{D(s)}, \tag{7}$$

$$\frac{V_{LP}}{V_{id}} = \frac{V_{O7} - V_{O8}}{V_{id}} = \frac{\left(\frac{G_{m1} G_{m4} G_{m5} R}{C_1 C_2}\right)}{D(s)} \tag{8}$$

where

$$D(s) = s^2 + s\frac{G_{m3} G_{m4} R}{C_1} + \frac{G_{m2} G_{m4} G_{m5} R}{C_1 C_2}. \tag{9}$$

Thus the filter realizes the voltage mode high-pass, band-pass and low-pass characteristics as exhibited from equations (6), (7) and (8) respectively. These expressions show the gain constants H_{HP}, H_{BP} and H_{LP} as below

$$H_{HP} = G_{m1} R, \quad H_{BP} = \frac{G_{m1}}{G_{m3}}, \quad H_{LP} = \frac{G_{m1}}{G_{m2}}. \tag{10}$$

The parameters pole-ω_o and pole –Q can be respectively expressed as

$$\omega_0 = \sqrt{\frac{G_{m2} G_{m4} G_{m5} R}{C_1 C_2}}, \tag{11}$$

$$Q = \frac{1}{G_{m3}} \sqrt{\frac{G_{m2} G_{m5} C_1}{G_{m4} C_2 R}}. \tag{12}$$

The pole- ω_o and pole-Q sensitivities are

$$S_{C_1 C_2}^{\omega_0} = -\frac{1}{2}, \quad S_R^{\omega_0} = \frac{1}{2},$$

$$S_{C_1}^{Q} = \frac{1}{2}, \quad S_{C_2}^{Q} = -\frac{1}{2}, \quad S_R^{Q} = -\frac{1}{2}. \tag{13}$$

It is evident from (13) that the realized filter exhibits low sensitivity for the parameters of interest.

Assuming $G_{m4} = G_{m5} = G_m$ and $C_1 = C_2 = C$, equations (11) and (12) respectively reduce to

$$\omega_0 = \frac{G_m}{C} \sqrt{G_{m2} R}, \tag{14}$$

$$Q = \frac{1}{G_{m3}} \sqrt{\frac{G_{m2}}{R}}. \tag{15}$$

From equations (14) and (15), it is clear that the pole-ω_o and pole-Q can be independently controlled by digitally changing the programmable transconductance G_m and G_{m3}.

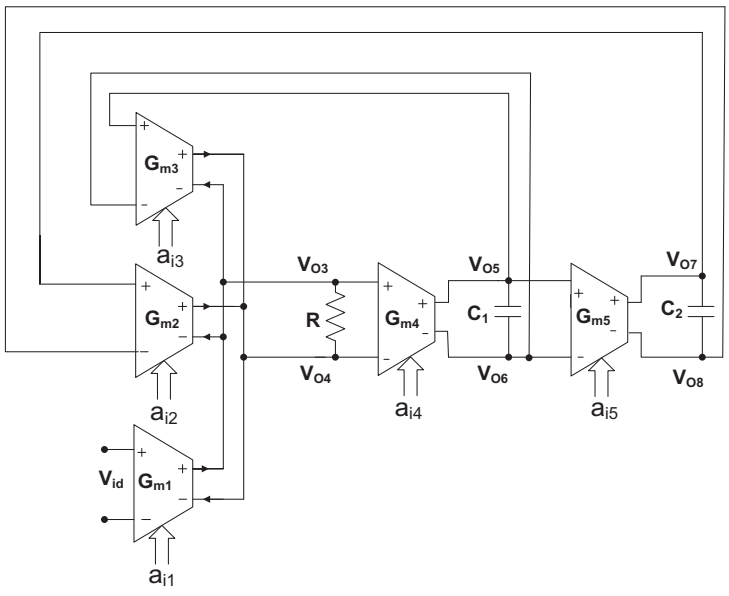

Fig. 6. Proposed digitally programmable fully differential KHN filter.

3. Effect of DCBOTA Non-idealities and Parasitic Output Resistances

3.1 Effect of Non-idealities

This subsection deals with the non-ideal analysis of the circuit proposed in Section 2. The transconductance gain of the OTA [18] with the non-idealities can be assumed as

$$G_{mni} \cong G_{mi}\left(1-\mu_i s\right)\left(i=1-5\right) \tag{16}$$

where $\mu_i = (1 / \omega_{Gi})$ and ω_{Gi} is the first pole of the OTA$_i$ (i = 1 – 5). Using (16) the ideal transfer functions of the second order HP, BP and LP filter sections given in equations (6), (7) and (8) respectively, yields the following non-ideal transfer functions.

$$\frac{V_{HP}}{V_{in}} \cong \frac{s^2 R G_{m1}\left(1-\mu_1 s\right)}{D(s)}, \tag{17}$$

$$\frac{V_{BP}}{V_{in}} \cong \frac{\dfrac{sRG_{m1}G_{m4}}{C_1}\left\{1-\left[\left(\mu_1+\mu_4\right)s-\mu_1\mu_4 s^2\right]\right\}}{D(s)}, \tag{18}$$

$$\begin{aligned}\frac{V_{LP}}{V_{in}}\Bigg| &\cong \frac{\dfrac{sRG_{m1}G_{m4}G_{m5}}{C_1C_2}\left[1-\left(\mu_1+\mu_4+\mu_5\right)s\right]}{D(s)} \\ &+\frac{\dfrac{sRG_{m1}G_{m4}G_{m5}}{C_1C_2}\left[\left(\mu_1\mu_4+\mu_1\mu_5+\mu_4\mu_5\right)s^2\right]}{D(s)} \\ &-\frac{\dfrac{sRG_{m1}G_{m4}G_{m5}}{C_1C_2}\left[\left(\mu_1\mu_4\mu_5\right)s^3\right]}{D(s)}\end{aligned} \tag{19}$$

where

$$\begin{aligned}D(s)\Big| &\cong s^2+\frac{sRG_{m3}G_{m4}}{C_1}\left\{1-\left[\left(\mu_3+\mu_4\right)s-\mu_3\mu_4 s^2\right]\right\} \\ &+\frac{RG_{m2}G_{m4}G_{m5}}{C_1C_2}\left[1-\left(\mu_2+\mu_4+\mu_5\right)s\right] \\ &+\frac{RG_{m2}G_{m4}G_{m5}}{C_1C_2}\left[\left(\mu_2\mu_4+\mu_2\mu_5+\mu_4\mu_5\right)s^2\right] \\ &-\frac{RG_{m2}G_{m4}G_{m5}}{C_1C_2}\mu_2\mu_4\mu_5 s^3.\end{aligned} \tag{20}$$

Due to non-idealities of the OTAs the HP, BP and LP responses deviate from the ideal responses. But the parasitic effect can be made negligible by satisfying the following conditions

$$\begin{aligned}&1 \gg \mu_1 s; \\ &1 \gg \left[\left(\mu_1+\mu_4\right)s-\mu_1\mu_4 s^2\right]; \\ &1 \gg \left[\left(\mu_1+\mu_4+\mu_5\right)s-\left(\mu_1\mu_4+\mu_1\mu_5+\mu_4\mu_5\right)s^2+\mu_1\mu_4\mu_5 s^3\right]; \\ &1 \gg \left[\left(\mu_3+\mu_4\right)s-\mu_3\mu_4 s^2\right]; \\ &1 \gg \left[\left(\mu_2+\mu_4+\mu_5\right)s-\left(\mu_2\mu_4+\mu_2\mu_5+\mu_4\mu_5\right)s^2+\mu_2\mu_4\mu_5 s^3\right]\end{aligned} \tag{21}$$

3.2 Effect of DCBOTA Parasitic Output Resistances

This subsection explores the effect of device output parasitic resistances on the performance of the proposed circuit. Within the scope of effect of these parasitic elements, the proposed digitally programmable fully differential KHN filter as depicted in Fig. 6 can be modified as shown in Fig. 7 in which the parasitics are R_{XP} and R_X. It may be noted that the output resistance of DCBOTA is assumed as R_O. Here $R_{XP} = R_O/3$ and $R_X = R_O$.

Analysis of the filter (Fig. 7) by taking into account the parasitic effects results in the following modified transfer functions

$$\begin{aligned}\frac{V_{HP}}{V_{id}}\Bigg| &= \frac{V_{03}-V_{04}}{V_{id}} \\ &= \frac{s^2 G_{m1}Z+s\dfrac{G_{m1}Z}{2R_X}\left(\dfrac{C_1+C_2}{C_1C_2}\right)+\dfrac{G_{m1}Z}{4C_1C_2R_X^2}}{D(s)}\end{aligned} \tag{22}$$

$$\frac{V_{BP}}{V_{id}} = \frac{V_{05}-V_{06}}{V_{id}} = \frac{s\dfrac{G_{m1}G_{m4}Z}{C_1}+\dfrac{G_{m1}G_{m4}Z}{2R_XC_1C_2}}{D(s)}, \tag{23}$$

$$\begin{aligned}\frac{V_{LP}}{V_{id}}\Bigg| &= \frac{V_{07}-V_{08}}{V_{id}} \\ &= \frac{\dfrac{2G_{m5}R_X}{2sC_2R_X+\left[s\dfrac{G_{m1}G_{m4}Z}{C_1}+\dfrac{G_{m1}G_{m4}Z}{2C_1C_2R_X}\right]}}{D(s)},\end{aligned} \tag{24}$$

where

$$\begin{aligned}D(s)\Big| &= s^2+s\left[\frac{G_{m3}G_{m4}Z}{C_1}+\frac{\left(C_1+C_2\right)}{2C_1C_2R_X}\right] \\ &+\frac{G_{m2}G_{m4}G_{m5}Z}{C_1C_2}+\frac{G_{m3}G_{m4}Z}{2C_1C_2R_X}+\frac{1}{4C_1C_2R_X^2}\end{aligned} \tag{25}$$

and

$$Z = \frac{2R_{XP}R}{2R_{XP}+R}. \tag{26}$$

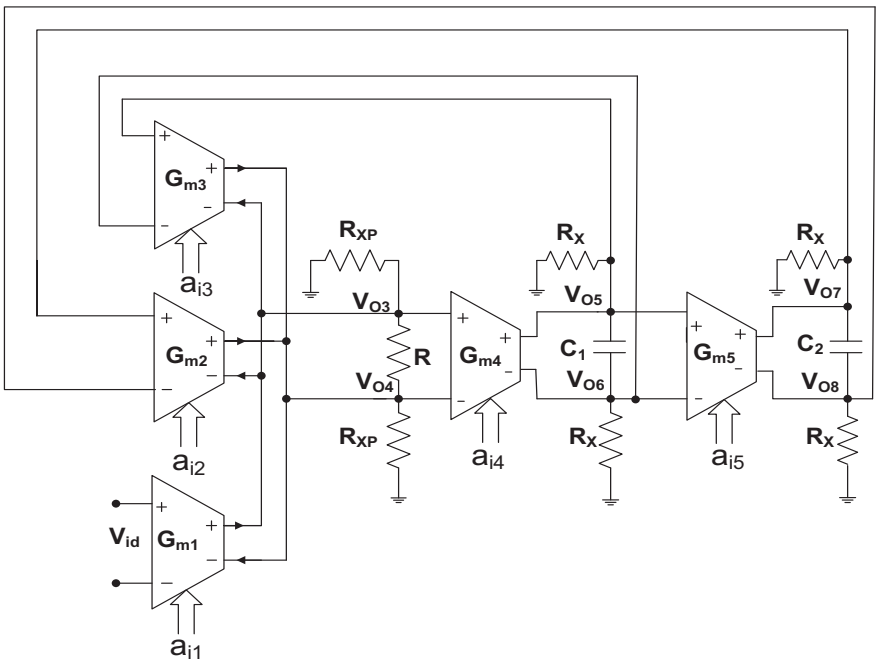

Fig. 7. Proposed digitally programmable fully differential KHN filter showing parasitic output resistances.

The pole-frequency and the quality factor of the proposed filter as a result of these parasitic elements are modified to

$$\omega_0' = \omega_0 \sqrt{k}, \tag{27}$$

$$Q' = Q \frac{R\sqrt{k}}{\left(\frac{C_1 + C_2}{2G_{m3}G_{m4}C_2R_X} + Z \right)}. \tag{28}$$

where

$$k = \left[\frac{Z}{R} + \frac{G_{m3}Z}{2G_{m2}G_{m5}R_X R} + \frac{1}{4G_{m2}G_{m4}G_{m5}R_X^2 R} \right]. \tag{29}$$

It is clear from (23), that the parasitic zero in band-pass transfer function significantly degrades the low frequency response.

From equations (22)-(24), the low-frequency gains ($\omega \rightarrow 0$) of high pass, band pass and low pass are

$$K_{HP}^0 = \frac{G_{m1}Z}{4G_{m2}G_{m4}G_{m5}RR_X^2 k}, \tag{30}$$

$$K_{BP}^0 = \frac{G_{m1}Z}{2G_{m2}G_{m5}RR_X k}, \tag{31}$$

$$K_{LP}^0 = \frac{G_{m1}Z}{G_{m2}Rk}. \tag{32}$$

Equations (30) and (31) indicate that when the frequency increases as a result of increasing G_{m4} and/or G_{m5}, the low-frequency gain of high-pass and band-pass decreases. Similarly, the low-frequency gain of low-pass filter as shown in equation 32, exhibits minimal variation only due to the presence of k. Thus it is clear that the band-pass response has finite attenuation at low frequencies as is also evident from Fig. 10.

4. Design and Verification

The design of the proposed filter (as shown in Fig. 6) was verified with values of $C_1 = C_2 = C = 10$ pF and $R = 10$ kΩ. The supply voltages were taken to be $V_{DD} = -V_{SS} = 1.5$ V and $V_C = -1.1$ V. Tab. 1 lists the variation of pole-frequency and pole-Q with control words a_{i4} and a_{i5} applied to DCBOTAs keeping control word a_{i2} constant. To make DC gain unity for LP, HP and BP, the digital control parameters corresponding to digital control word applied to the DCBOTAs are given in Tab. 2 for different frequencies. Fig. 8 shows the low pass responses at different frequencies which correspond to different control words listed in Tab. 1, each having a DC gain approximately equal to unity.

Tuning of high pass responses for the same control word is also depicted in Fig. 9, which also shows that the DC gain is unity. Both the low pass and high pass responses have the same pole frequencies. The band pass responses for the same control word applied to DCBOTAs for centre frequency 110 kHz, 508 kHz, 1.0 MHz and 3 MHz respectively are shown in Fig. 10 at a unity gain. The pole-Q variation by varying control word a_{i3} keeping a_{i2} = 11011111 and $a_{i4} = a_{i5}$ = 01001111 are also listed in Tab. 1 and the pole-Q variation for different control parameters at unity gain are given in Tab. 2. The curves A-D for different quality factors at a frequency of 1 MHz are shown in Fig. 11. The time domain response of the band pass filter shown in Fig. 12(a) is obtained by applying a differential sine wave of 1 V amplitude at 1 MHz. The Fourier spectrum of the band pass output signal, showing

Control word (a_{i2}) = 11011111 , Control word parameter (α_{i2}) = 0.871						
Curve	Control word (a_{i4}, a_{i5})	Control word parameter ($\alpha_{i4} = \alpha_{i5}$)	Frequency (KHz)	Control word (a_{i3})	Control word parameter (α_{i3})	Pole-Q
A	00000110	0.023	110	11111011	0.917	1
B	00100111	0.152	508	10000010	0.508	1.9
C	01001111	0.308	1000	01001100	0.281	3.5
D	11111111	0.996	3000	00101010	0.164	6

Tab 1. Variation of frequency with Control word for LP, HP and BP.

	Digital Control Parameters										
	Low-pass filter section/High pass filter section				Band-pass filter section				Pole-Q variation at 1MHz		
Curve	$\alpha_{1=}\alpha_2$	α_3	$\alpha_{4=}\alpha_5$	Frequency (*KHz*)	$\alpha_{1=}\alpha_3$	α_2	$\alpha_{4=}\alpha_5$	Frequency (*KHz*)	$\alpha_{1=}\alpha_3$	α_2	$\alpha_{4=}\alpha_5$
A	0.871	0.996	0.023	110	0.996	0.871	0.023	110	0.971	0.871	0.308
B	0.871	0.996	0.152	508	0.996	0.871	0.152	508	0.508	0.871	0.308
C	0.871	0.996	0.308	1000	0.996	0.871	0.308	1000	0.281	0.871	0.308
D	0.871	0.996	0.996	3000	0.996	0.871	0.996	3000	0.164	0.871	0.308

Tab 2. Variation of frequency with control word parameter for gain unity.

a good selectivity for the applied signal frequency of 1 MHz, is given in Fig. 12(b). The plot of Fig. 12(b) also shows harmonics occurring at high frequencies which are very obvious for band pass response. Fig. 13 shows Fourier spectrum of low-pass and high-pass output signal with THD of 1.8 % and 5.8 % respectively. The DC transfer characteristics for the low-pass output is consequently shown in Fig. 14 which suggests a linear variation of output for input in the range of –1 V to 1 V thus exhibiting a wide dynamic range. However, the effect of finite offset voltage is also visible from the characteristics.

Next the CMMR analysis [19], [20] of the proposed circuit is also performed. The fully differential nature of the circuit is especially desirable for rejection of common-mode signals. This is evident from the results of Fig. 15, which shows CMMR variation for low-pass output for curve B (Tab. 1b). Fig. 15 clearly shows very high CMMR, thus emphasizing the advantage of fully differential operation. The MOS transistor aspect ratios are given in Tab. 2. The device model parameters, used for the SPICE simulations are taken from MIETEC 0.5 µm CMOS process.

Transistor	Aspect ratio
M_1, M_2, M_3, M_4	22/6
M_5, M_6, M_7, M_8, M_9, M_{10}	80/2
M_{11}, M_{12}, M_{13}, M_{14}	160/2
M_{A1}, M_{A2}, M_{A3}, M_{A4}, M_{A5}, M_{A6}, M_{A7}	100/1

Tab 3. MOS Aspect ratios for DCBOTA.

5. Conclusion

In this paper a digitally programmable fully differential KHN filter has been presented with minimum passive components. The filter provides low pass, high pass and band pass responses simultaneously. The frequencies of the fully differential filter are digitally controlled by applying control words to DCBOTAs. The filter was designed at unity gain by proper selection of control words as depicted in Tab. 1. The frequency range covered by applying control words varies from 110 kHz to 3 MHz which shows a wide variation. The pole frequency and quality factor of the proposed filter can be independently controlled. Passive component sensitivities are also very low. The fully differential filter was designed and simulated using PSPICE.

References

[1] ALZAHER, H., ELWAN, H., ISMAIL, M. CMOS baseband filter for WCDMA integrated wireless receivers. *Electronics Letters*, 2000, vol. 38, no. 18, p. 1515 - 1516.

[2] IBRAHIM, A. M., KUNTMAN, H. A novel high CMRR high input impedance differential voltage-mode KHN-biquad employing DODDCCs. *International Journal of Electronics (AEU)*, 2004, vol. 58, p. 429 - 433.

[3] EL-ADAWY, A. A., SOLIMAN, A. M., ELWAN, H. O. A novel fully differential current conveyor and applications for analog VLSI. *IEEE Transactions on Circuits and Systems-II*, 2000, vol. 47, no. 4, p. 306 - 313.

[4] AL-SHAHRANI, S. M. Fully differential second order filter. In *Proceedings of the 47th IEEE International Midwest Symposium on Circuits and Systems (MWCAS)*. Hiroshima (Japan), 2004, vol. 3, p. 299 – 301.

[5] KAEWDANG, K., SURAKAMPONTOM, W. On the realization of electronically current-tunable CMOS OTA. *International Journal of Electronics and Communications*, 2007, vol. 61, p. 300 - 306.

[6] CHUNHUA, W., LING, Z., TAO, L. A new current OTA-C current mode biquad filter with single input and multiple outputs. *International Journal of Electronics and Communications*, 2008, vol. 62, p. 232 - 234.

[7] BIOLEK, D., BIOLKOVA, V., KOLKA, Z. Universal current-mode OTA-C KHN biquad. *World Academy of Science, Engineering and Technology*, 2007, vol. 31, p. 289 - 292.

[8] ZHANG, L., ZHANG, X., EL-MASRY, E. A highly linear bulk-driven CMOS OTA for continuous-time filters. *Analog Integrated Circuits and Signal Processing*, 2008, vol. 54, p. 229 - 236.

[9] SALAMA, K. N., SOLIMAN, A. M. Voltage-mode Kerwin-Huelsman-Newcomb circuit using CDBAs. *Frequenz*, 2000, vol. 54, p. 90 - 93.

[10] MAHESHWARI, S. Analog signal processing applications using a new circuit topology. *IET Circuits, Devices and Systems*, 2009, vol. 3, p. 106 -115.

[11] SALAMA, K. N., SOLIMAN, A. M. CMOS operational transresistance amplifier for analog signal processing. *Microelectronics Journal*, vol. 30, no. 3, 1999, p. 235 - 245.

[12] HASHIESH, M. A., MAHMOUD, S. A., SOLIMAN, A. M. Digitally controlled CMOS balanced output transconductor based on novel current-division network and its application. In *Proceedings of the 47th IEEE International Midwest Symposium on Circuits and Systems (MWCAS)*. Hiroshima (Japan), 2004, vol. III, p. 323- 326.

[13] HASSAN, T. M., MAHMOUD, S. A. Low-voltage digitally programmable band-pass filter with independent controls. In *Proceedings of the IEEE International Conference on Signal Processing and Communications (ICSPC 2007)*. Dubai (UAE), 2007, p. 24 -27.

[14] MAHMOUD, S. A., AWAD, I. A. New CMOS balanced output transconductor and application to *Gm*-C biquad filter. In *Proceedings of the IEEE International Symposium on Circuits and Systems*. Bangkok (Thailand), 2003, vol. 1, p. 385 - 388.

[15] TANGSRIRAT, W. Low-voltage digitally programmable current mode universal biquadratic filter. *International Journal of Communication (AEU)*, 2008, vol. 62, p. 97 - 103.

[16] ALZAHER, H. A., TASADDUQ, N. A. A digitally programmable polyphase filter for Bluetooth. *International Conference on Mixed Design of Integrated Circuits & Systems (MIXDES 2009)*. Warsaw (Poland), 2009, p.592 – 596.

[17] TANGSRIRAT, W., PRASERTSOM, D., SURKAMPONTORN, W. Low-voltage digitally controlled current differencing buffered amplifier and its application. *International Journal of Electronics and Communication*, 2009, vol. 63, p. 249 - 258.

[18] TSUKUTANI, T., HIGASHIMURA, M., TAKAHASHI, N., SUMI, Y., FUKUI, Y. Versatile voltage-mode active-only biquad with lossless and lossy integrator loop. *International Journal of Electronic*, 2001, vol. 88, p. 1093 - 1102.

[19] MAHESHWARI, S. High CMMR wide bandwidth instrumentation amplifier using controlled conveyors. *International Journal of Electronics*, 2002, vol. 89, no.12, p.889 - 896.

[20] CASAS, O., PALLAS-ARENY, R. Basics of analog differential filters. *IEEE Transactions on Instrumentation and Measurement*, 1996, vol. 45, no. 1, p. 977 - 985.

About the Authors …

Parveen BEG is a Lecturer in the Department of Electronics Engineering, Zakir Hussain College of Engineering and Technology, Aligarh Muslim University (AMU), India. She received her B.Sc and M.Sc (Hons.) degrees in Electronics Engineering from AMU in 1999 and 2002 respectively. Her research interests include analysis and design of circuits and systems, system design and modeling and she has published 12 papers in reputed Journals and National/International Conferences.

Iqbal A. KHAN received his B.Sc Engg., M.Sc. Engg., and PhD degrees in Electrical Engineering, all from Aligarh Muslim University, Aligarh, India in 1976, 1978 and 1987 respectively. He joined the Department of Electrical Engineering, Aligarh Muslim University in 1979 as a Lecturer and was subsequently appointed as Reader in the Department of Electronics at the same university in 1987. He became a Professor in the same department in 1998. Recently, he joined as Professor at the Department of Electrical Engineering, Faculty of Engineering and Islamic Architecture, Kingdom of Saudi Arabia. He teaches and conducts research in VLSI circuits and systems, filter theory and design, digital systems and electronic instrumentation. He has supervised 40 Masters dissertations, 5 PhD theses and has published over 100 technical papers in international journals and conference proceedings. He is Life Fellow of the Institution of Electronics and Telecommunication Engineers, India, Life Member of Systems Society of India and Senior Member of the IEEE.

Sudhanshu MAHESHWARI obtained his B.Sc. (Engg.), M. Tech and Ph.D degrees from Aligarh Muslim University in 1992, 1999 and 2004 respectively. He is currently Associate Professor in the Department of Electronics Engg., Aligarh Muslim University, India. He has been engaged in teaching and design of courses related to the design and synthesis of Analog Electronic Circuits and Current-mode Circuits. His research areas include analog signal processing circuits and current-mode circuits. He has published more than 70 research papers, including more than 50 international journal papers. He has also been on the reviewer panel for several top ranked international journals.

Muzaffer A. SIDDIQI received his BSc. degree in Electrical Engineering in 1968, MSc Engg. in 1973 and Ph.D. in 1979, all from Aligarh Muslim University (AMU), Aligarh, India. He is presently a Professor of Electronics Engg. at AMU, Aligarh, where he has been associated with teaching and research work since 1970. His research interests include active network synthesis, specially active-R, Active-C circuits and computer aided design. Dr. Siddiqi has supervised a large number of UG and PG projects at AMU, Aligarh, Jamia Al-Fateh, Libya and has published 26 technical papers in reputed journals and in national/international conferences. His present interests include VLSI design, semiconductor memories and current mode analog circuit design.

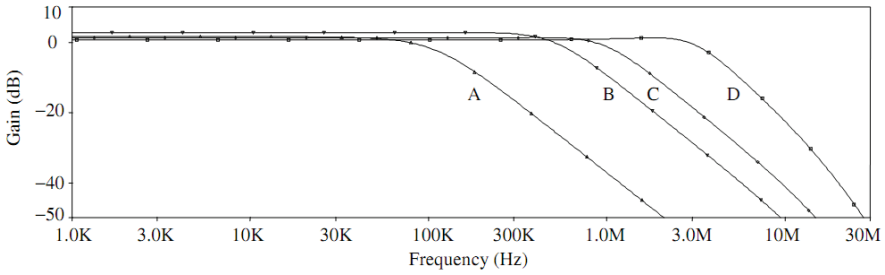

Fig. 8. Tuning of low-pass filter function with digital control word.

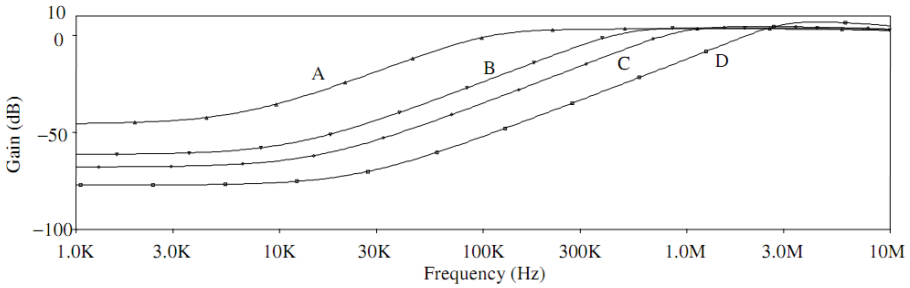

Fig. 9. Tuning of high-pass filter function with digital control word.

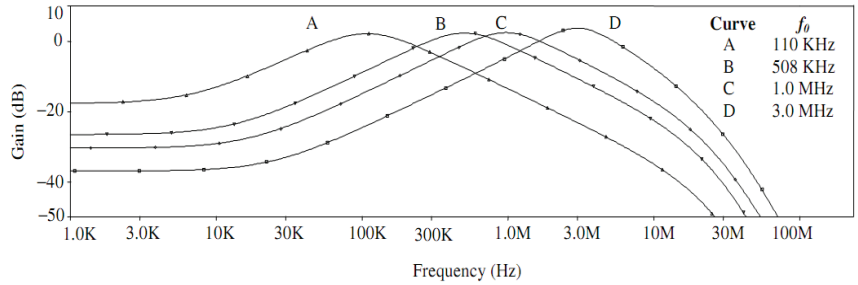

Fig. 10. Tuning of band-pass filter function with digital control word.

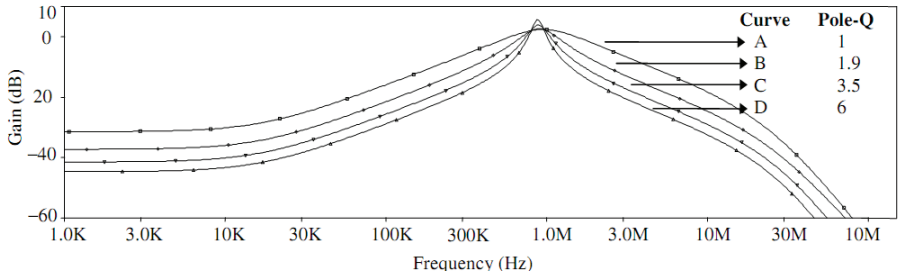

Fig. 11. Pole-Q variations with digital control word.

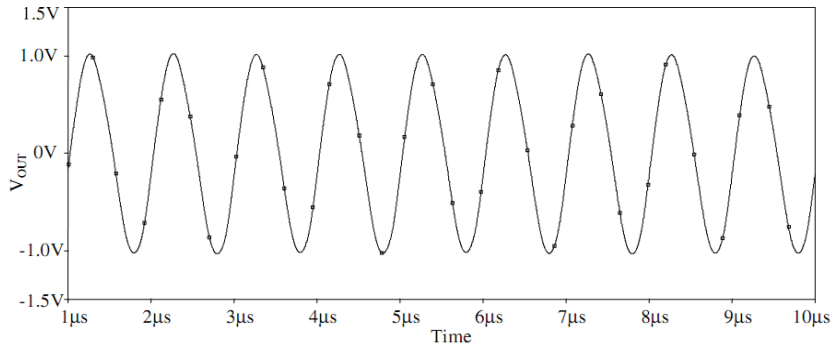

Fig. 12(a). Output waveform of the band-pass filter for a 1 V sinusoidal differential input voltage at 1 MHz.

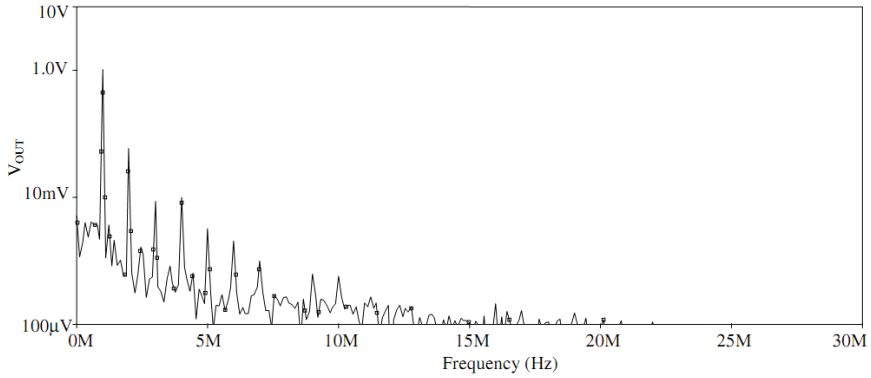

Fig. 12(b). Fourier spectrum of band-pass output signal.

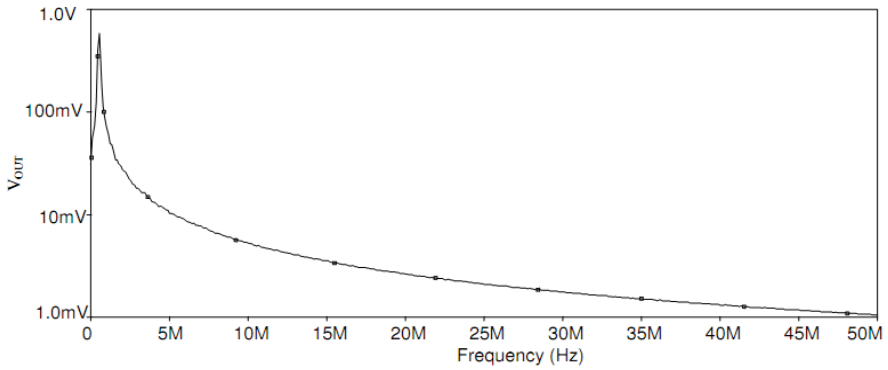

Fig. 13(a). Fourier spectrum of low-pass output signal.

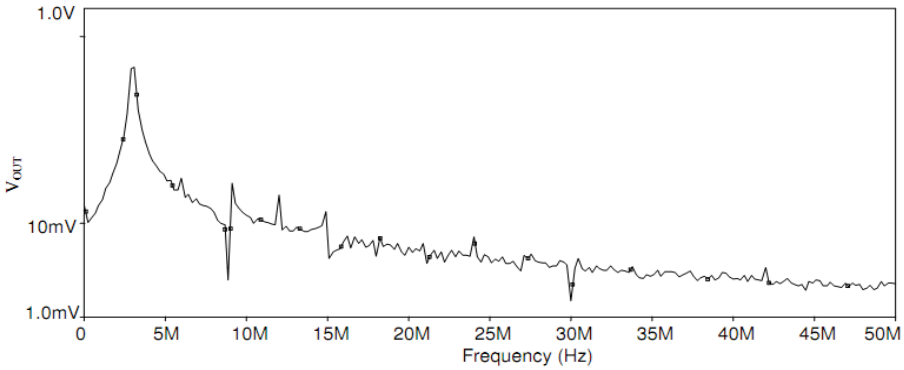

Fig. 13(b). Fourier spectrum of high-pass output signal.

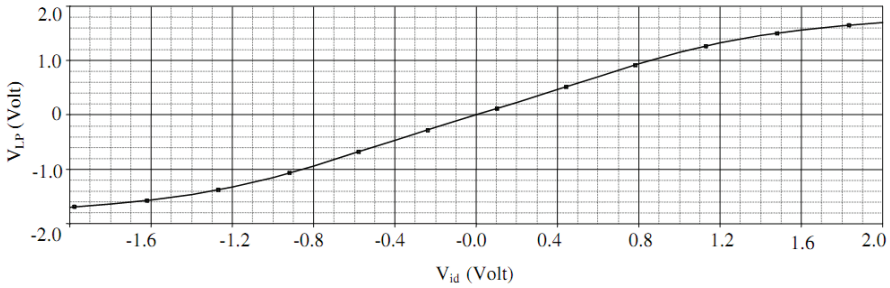

Fig. 14. DC transfer characteristic of low-pass output.

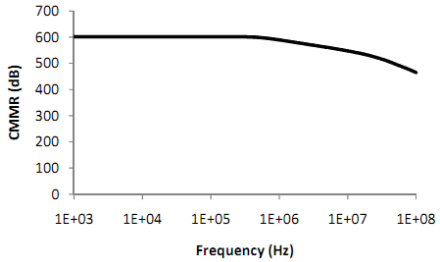

Fig. 15. CMMR frequency response of the low-pass filter for curve B.